Biochimie 142 (2017) 197–206

Contents lists available at ScienceDirect

Biochimie

journal homepage: www.elsevier.com/locate/biochi

Research paper

Selectin-independent adhesion during ovarian cancer metastasis

Nadezhda A. Khaustova [a, 1], Diana V. Maltseva [a, *, 1], Leticia Oliveira-Ferrer [b], Christine Stürken [c], Karin Milde-Langosch [b], Julia A. Makarova [d], Sergey Rodin [a, e], Udo Schumacher [c], Alexander G. Tonevitsky [d]

[a] SRC Bioclinicum, Moscow, 115088, Russia
[b] Department of Gynecology, University Medical Center Hamburg-Eppendorf, Hamburg, D-20246, Germany
[c] Department of Anatomy and Experimental Morphology, University Medical Center Hamburg-Eppendorf, Hamburg, D-20246, Germany
[d] P. Herzen Moscow Oncology Research Institute, Moscow, 125284, Russia
[e] Department of Medical Biochemistry and Biophysics, Karolinska Institutet, 17177, Stockholm, Sweden

ARTICLE INFO

Article history:
Received 26 May 2017
Accepted 12 September 2017
Available online 14 September 2017

Keywords:
Ovarian cancer
Metastasis
Selectin
Tumor cell adhesion
Integrin
Laminin

ABSTRACT

Purpose: Ovarian cancer (OvCa) progression mainly takes place by intraperitoneal spread. Adhesion of tumor cells to the mesothelial cells which form the inner surface of the peritoneum is a crucial step in this process. Cancer cells use in principle different molecules of the leukocyte adhesion cascade to facilitate adhesion. This cascade is initiated by selectin-ligand interactions followed by integrin - extracellular matrix protein interactions. Here we address the question whether all tumor cells predominantly employ selectin-dependent leukocyte-like adhesion cascade (SDAC) or whether they use integrin mediated adhesion for OvCa progression as well.

Methods: A comparative transcriptomic analysis of the human OvCa cell lines OVCAR8 and SKOV3 was performed. Intraperitoneal xenograft model of OVCAR8 cells was used to determine whether there is a correlation between SDAC gene expression and the metastatic potential of the control cells and the cells overexpressing c-Fos. Transcriptomic analysis of OVCAR8 and SKOV3 samples was performed using microarrays.

Results: One-third of the protein-coding genes involved in SDAC exhibited lower expression levels in OVCAR8 than in SKOV3 cells. In contrast to SKOV3 cells, c-Fos overexpression in OVCAR8 cells did not significantly influence the expression of SDAC genes. Intraperitoneal xenograft model of OVCAR8 cells unexpectedly demonstrated that the aggressiveness of OVCAR8 tumors was not depended on the c-Fos expression level and was comparable to that of SKOV3 control tumors. Gene expression analysis of tumors suggests that SKOV3-derived tumor progression was mainly depended on SDAC. Progression of OVCAR8 tumors relied on other cell adhesion molecules that do not interact with selectins.

Conclusions: High expression of c-Fos in ovarian cancer cells is not always associated with reduced metastatic potential. Low expression level of SDAC genes may not ensure low OvCa metastatic potential hence alternative adhesion mechanisms involving laminin-integrin interactions exist as well.

1. Introduction

The E- and P-selectin-dependent leukocyte-like adhesion cascade (SDAC) of tumor cells is considered a standard mechanism of extravasation during metastasis formation [1–4]. The cascade is divided into three sequential steps. The first step is the capturing and rolling of tumor cells on the endothelial surface. The second step is cellular arrest and tight attachment to the endothelial cells. The third step is diapedesis or abrogation of endothelial integrity and active transmigration through the endothelial barrier into the

Abbreviations: OvCa, ovarian cancer; c-Fos, a transcription factor of the activating protein-1 (AP-1) family; OVCAR8-*c*-Fos, OVCAR8 cells overexpressing c-Fos; SKOV3-*c*-Fos, SKOV3 cells overexpressing c-Fos; SDAC, selectin-dependent leukocyte-like adhesion cascade.

* Corresponding author.
E-mail addresses: khaunadia@gmail.com (N.A. Khaustova), d.maltseva@bioclinicum.com (D.V. Maltseva), ferrer@uke.de (L. Oliveira-Ferrer), c.stuerken@uke.de (C. Stürken), milde@uke.de (K. Milde-Langosch), j-makarova@ya.ru (J.A. Makarova), sergey.rodin@ki.se (S. Rodin), uschumac@uke.de (U. Schumacher), tonevitsky@mail.ru (A.G. Tonevitsky).
[1] These authors contributed equally.

https://doi.org/10.1016/j.biochi.2017.09.009
0300-9084/

tissues. The first and most crucial step is mainly mediated by selectins [1,5–7]. Selectins are a family of transmembrane cell adhesion glycoproteins. While stimulated endothelial and mesothelial cells express E- and P-selectins, tumor cells express their respective ligands [4,8,9]. Although other cell adhesion molecules such as integrins, cadherins, and galectins are also involved in tumor cell adhesion, selectins are still regarded as the most important molecules for the first step of the adhesion cascade. Ovarian cancer progression mainly occurs by intraperitoneal metastasis facilitated by the circulation of peritoneal fluid [10]. As in the case of hematogenous metastasis, one of the most crucial steps of the process is an attachment of tumor cells to the peritoneal mesothelium. Potential mechanisms may include binding of tumor cells both to selectins [9] and to extracellular matrix proteins expressed on the surface of human peritoneal mesothelial cells via integrins [10–12]. Whether all tumor cells employ solely selectin-dependent adhesion to metastasize or whether additional cell adhesion molecules play an important role is not yet clearly defined.

High expression of the transcription factor c-Fos, a known oncogene, is associated with good prognoses in ovarian cancer (OvCa) patients [13]. We recently showed that one possible reason for the good prognosis is a change in tumor cell adhesion properties [15]. Thus, stable c-Fos overexpression in the human OvCa cell lines SKOV3 and OVCAR8 is associated with reduced adhesion of both types of OvCa cells to extracellular matrix components and E-selectin as well as to mesothelial and endothelial cells in *in vitro* assays. Compared with control SKOV3 cells c-Fos overexpression in SKOV3 cells transplanted in an intraperitoneal xenograft model leads to higher overall survival of the mice, a decrease in the number of circulating tumor cells (CTCs), and inhibition of tumor growth and lung metastasis formation [15].

In the present study, we investigated the influence of c-Fos overexpression on the transcriptome and the *in vivo* metastatic potential of OVCAR8 cells in comparison with similar previously obtained data for SKOV3 cells. The comparative transcriptomic analysis of OVCAR8 and SKOV3 cells revealed that in cultured control OVCAR8 cells one-third of the SDAC genes exhibit lower expression levels as compared to that in cultured control SKOV3 cells. In contrast to SKOV3, c-Fos overexpression in OVCAR8 cells does not significantly influence expression of the SDAC genes; the levels of these genes in OVCAR8 cells overexpressing c-Fos are similar to those of control OVCAR8 cells. We used an intraperitoneal xenograft model of OVCAR8 cells to determine whether there was a correlation between the SDAC gene expression and the metastatic potential of the OvCa cells with and without c-Fos overexpression. We showed that the aggressiveness of OVCAR8-derived tumors is not dependent on the c-Fos expression level and is comparable to that of SKOV3 control tumors. Our results suggest that OvCa cells might use a selectin-independent mechanism of the initial attachment to peritoneal mesothelium.

2. Materials and methods

2.1. Cell lines

All cells derived from the human OvCa cell line OVCAR8 were cultivated as described in Ref. [11,14]. Stable clones overexpressing c-Fos were generated as described in Ref. [15] by performing transfections with the plasmid c-Fos-pIRES-P containing the full-length c-Fos cDNA cloned in the bicistronic vector pIRES-P. Transfectants with the empty vector were used as negative controls. The differences in c-Fos expression were confirmed by western blotting. For the following xenograft experiment, OVCAR8-*c*-Fos and OVCAR8-pIRES-P (OVCAR8-NC, negative control) cells were used.

2.2. Intraperitoneal xenograft mouse model

Animal experiments were conducted according to the UKCCR guidelines for the welfare of animals in experimental neoplasia [16]. For injection into SCID mice, OVCAR8-NC and OVCAR8-*c*-Fos cells were suspended in RPMI medium at a concentration of 5 x 10^6 ml^{-1}. A total of 200 μl of that suspension was injected into the peritoneal cavity of female mice (10 animals per group). Mice that showed strong signs of tumor progression (ascites, shaggy coat and loss of appetite [16]) were sacrificed. Primary tumors were removed, weighed and processed for histological analysis, RNA isolation, and protein isolation. Peritoneal metastases were excised, counted, frozen or formalin fixed, and embedded in paraffin. Right lungs were excised en bloc and prepared for histological analysis; left lungs were subjected to DNA isolation. Bone marrow samples were obtained by flushing the left femora with 1 ml of 0.9% NaCl. The bone marrow suspension and 200 μl of blood were also subjected to DNA isolation.

2.3. DNA extraction and real-time PCR for the detection of circulating and disseminated tumor cells

DNA was extracted from 200 μl of murine blood using the QIAamp DNA Blood Mini Kit (Qiagen, Hilden, Germany). For DNA isolation from murine bone marrow and lungs, the QIAamp DNA Mini Kit (Qiagen, Hilden, Germany) was used according to the manufacturer's instructions. A standard range with a 10-fold dilution of extracted DNA from 1×10^6 cultured OVCAR8 cells to one cell was established. Control samples were isolated from mice without injected tumor cells. To quantify human tumor cells by real-time polymerase chain reaction (PCR), established primers specific for human ALU sequences were used as described in Ref. [17]. Analyses were performed in triplicate and in at least two independent experiments for each sample.

2.4. RNA isolation and cDNA microarray analysis

Approximately 50 mg of flash-frozen OVCAR8 control and c-Fos-overexpressed primary tumor tissue was used. RNA isolation and quality controls were performed as described in Ref. [18]. The RNA integrity number (RIN) values ranged from 6.8 to 8.7. Procedures for cDNA synthesis and labelling were carried out according to the Ambion WT Expression Kit (Life Technologies, Darmstadt, Germany) using 500 ng of total RNA as the starting material. These experiments were performed using the Affymetrix Human Gene 1.0 ST Array (Affymetrix Inc., Santa Clara, CA, USA) according to the manufacturer's instructions (Affymetrix Manual P/N 701880 Rev. 4) and as described elsewhere [19]. The raw microarray data deposited in NCBI's Gene Expression Omnibus and are accessible through GEO Series accession number GSE97226 (https://www.ncbi.nlm.nih.gov/geo/query/acc.cgi?acc=GSE97226).

2.5. Microarray data processing and bioinformatic analysis

Human Gene 1.0 ST microarray data were processed using the Affymetrix Expression Console (build 1.4.1.46) [20] implementation of the Robust Multichip Average (RMA) method [21]. The processing microarray data are described in detail in Refs. [19,22]. For the detection of differentially expressed genes, the threshold for the adjusted p-value was set at 0.05, and the threshold for the fold change (FC) was set at 1.5.

Bioinformatic analysis was performed using the DAVID online tool (https://david.ncifcrf.gov/, version 6.8). All of the analyzed genes were classified into several functional groups. The p-values on the tabs are modified Fisher's exact p-values. When members of

two independent groups can fall into one of two mutually exclusive categories, Fisher's exact test is used to determine whether the proportions of those falling into each category differ by group. In the DAVID annotation system, Fisher's exact test is used to measure the gene enrichment in annotation terms. For bioinformatic analysis, we used only genes with expression levels of 100 Affymetrix expression units (baseline threshold) or more.

3. Results

3.1. c-Fos overexpression does not affect metastasis in an intraperitoneal xenograft model of OVCAR8 cells

To investigate the effects of c-Fos on tumor growth *in vivo*, we injected control unmodified OVCAR8 (OVCAR8-NC) cells and OVCAR8 cells overexpressing c-Fos (OVCAR8-*c*-Fos cells) intraperitoneally into SCID mice (10 mice per group). In contrast to our earlier published data on SKOV3-derived tumors [15], c-Fos overexpression in OVCAR8 cells did not inhibit the development of cancer *in vivo* (Table 1). There was no statistically significant difference in the overall survival between OVCAR8-NC- and OVCAR8-*c*-Fos-injected mice. The average weight of primary OVCAR8-*c*-Fos tumors was quite higher than that of control OVCAR8-NC tumors, but the changes were not statistically significant. We also quantified CTCs and disseminated tumor cells (DTCs) in the blood, lungs and bone marrow using *Alu*-PCR. The average numbers of CTCs per ml of blood and DTCs per gram of lung and bone marrow tissue were even higher in OVCAR8-*c*-Fos mice than in control mice. Thus, despite the reduction in adhesion properties observed in the *in vitro* assays of OVCAR8 cells in response to c-Fos overexpression [15], the metastatic potential of OVCAR8-*c*-Fos cells *in vivo* was not inhibited.

3.2. Comparison of transcriptomes from OVCAR8 and SKOV3 samples

To reveal the possible causes of the different effects of c-Fos overexpression in OVCAR8-and SKOV3-derived tumors, we performed a microarray analysis of OVCAR8-derived control and c-Fos-overexpressed tumors. We also reanalyzed total RNA samples previously isolated from SKOV3 control and c-Fos-overexpressed cells [15] using the same type of microarrays. Then, we combined and simultaneously analyzed the OVCAR8 tumor microarray data, SKOV3 cell microarray data and previously obtained data for OVCAR8 cells and SKOV3 tumors [15].

Table 1
Tumor growth and metastasis after intraperitoneal injection of OVCAR8 cells into SCID mice.

Characteristic	OVCAR8-NC	OVCAR8-*c*-Fos
Survival (days)	40.2 ± 6.6	46.6 ± 0.5
Primary tumor[a]	7/7[b]	5/5[b]
Peritoneal metastasis	7/7[b]	5/5[b]
Primary tumor weight (g)	<0.02 g	0.4 ± 0.6 g
Ascites	0/7 (0%)	2/5 (40%)
CTCs/ml blood	5768 ± 3045	8229 ± 3006
DTC/lung	37 ± 6	107 ± 5
DTC/BM	52 ± 22	737 ± 324

Values ± SE.
NC: non-treated control.
CTCs: circulating tumor cells.
DTCs: disseminated tumor cells.
BM: bone marrow.
[a] Tumor at the injection site.
[b] The rest of the animals (a total of 10) were found dead and could not be analyzed.

Together our present and previous results show that c-Fos overexpression causes changes in the expression levels of hundreds of genes in both types of cells and tumors. To identify potential pathways responsible for the different responses of OVCAR8 and SKOV3 tumors to c-Fos overexpression, we compared the transcriptome profiles of c-Fos-overexpressing OVCAR8 cells and tumors with those of SKOV3 samples. In particular, we identified 410 genes with 5-fold or larger differences in expression between OVCAR8-*c*-Fos tumors and SKOV3-*c*-Fos tumors. In the cell samples, we identified 347 such genes. Both mRNA lists were analyzed to detect enriched metabolic pathways. The pathways identified are listed in Table 2 and include cell adhesion, glycoproteins, extracellular matrix organization, extracellular space, and membrane proteins.

3.3. Deregulation of genes encoding proteins involved in the selectin-dependent leukocyte-like adhesion cascade

Taking advantage of the combined analysis of the OVCAR8 tumor and SKOV3 cell transcriptome data and the previously obtained data from OVCAR8 cells and SKOV3 tumors [15], we observed that 44% of the protein-coding mRNAs involved in the SDAC are downregulated up to 12-fold in cultured SKOV3 cells in response to c-Fos overexpression (see Additional file 1: Table S1). Consistent with this finding, significantly reduced adhesion of cultured SKOV3-*c*-Fos cells to E-selectin has also been demonstrated [15]. SKOV3-derived tumors showed a similar response to c-Fos overexpression and exhibited an up to 46-fold decrease in the expression of genes from the SDAC (Fig. 1). In particular, the gene expression levels of known E- and P-selectin ligands carrying glycoproteins such as *CD44, MUC1, CD24,* and *PODXL* [2,7,23–27] were reduced 1.5-fold or more in the SKOV3-derived tumors compared with control tumors.

Cultured OVCAR8 cells exhibited lower sensitivity in response to c-Fos overexpression. Remarkably, the microarray data analysis revealed that only 15% of the genes in the SDAC were downregulated. OVCAR8-derived tumors exhibited a significant decrease (more than 1.5 times lower) in the expression of only one gene (*CD24*) from the selectin ligands and other one (*PODXL*) even was increased. It should be noted that 40% of the genes from the SDAC exhibited lower expression levels (up to 147 times lower) in control OVCAR8 tumors than in control SKOV3 tumors (see Additional file

Table 2
Pathway analysis of mRNAs differentially expressed in OVCAR8-and SKOV3-*c*-Fos-overexpressed samples.

Pathway	Number of genes	Adjusted p-value
Tumors		
Cell adhesion	40	3,8E-13
Glycoprotein	140	7,6E-11
Signal	128	1,1E-9
Glycosylation site: N-linked (GlcNAc …)	125	1,1E-6
Calcium ion binding	39	3,8E-6
Cadherin	15	6,6E-6
Secreted	68	5,1E-6
Extracellular matrix organization	19	2,7E-5
Extracellular space	52	1,8E-4
Membrane	166	3,6E-3
Cells		
Cell adhesion	29	1,0E-9
Signal	85	1,1E-5
Glycoprotein	91	1,1E-5
Calcium ion binding	26	3,9E-3
Cadherin	10	3,1E-3
Membrane	116	1,7E-2
Secreted	41	2,2E-2
Extracellular space	35	2,3E-2

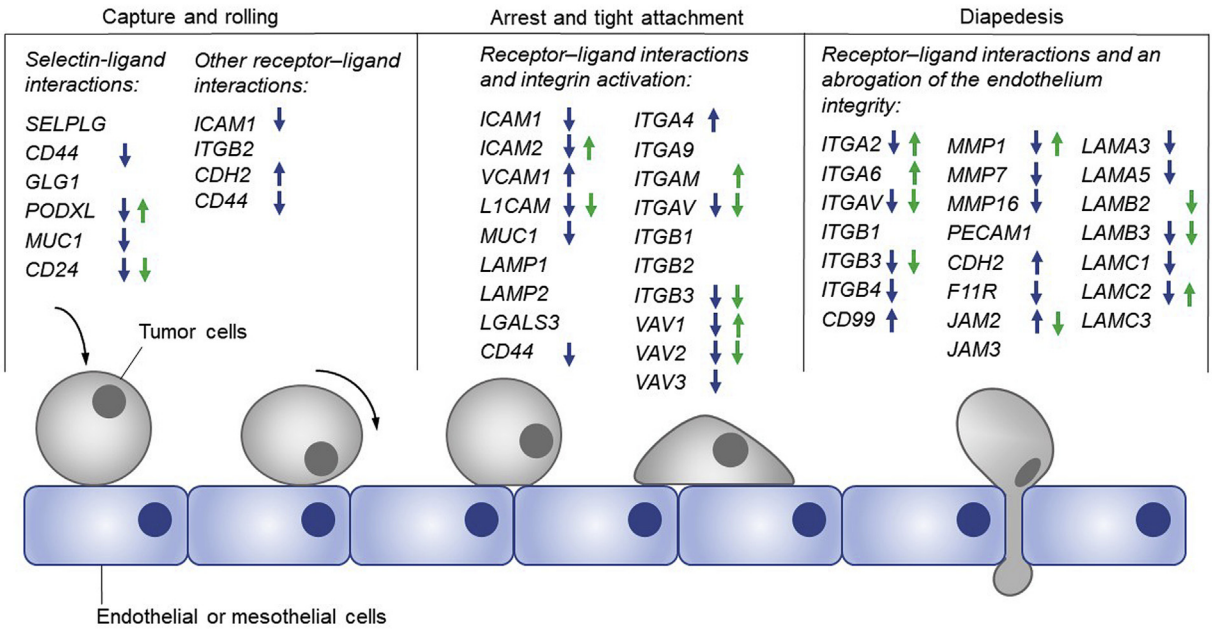

Fig. 1. Three sequential steps of the selectin-dependent leukocyte-like adhesion cascade of tumor cells during metastasis. Arrows mark downregulated or upregulated genes encoding proteins involved in the cascade in response to c-Fos overexpression in SKOV3- (in blue) or OVCAR8-derived (in green) tumors.

2: Table S2), and c-Fos overexpression reduced that number to 20%. However, in both cultured cells and tumor samples with and without c-Fos overexpression, 15–25% of the genes from the cascade had higher expression levels in OVCAR8 samples (up to 10 times higher) than in SKOV3 samples. This group of genes included many genes that are involved in the second and third steps of the cascade (e.g., *ICAM1*, *ICAM2*, *LAMA1*, *LAMB2*, and *JAM2*).

3.4. Deregulation of genes encoding glycosylation enzymes

A prerequisite for E-selectin-dependent adhesion is the glycosylation of cell surface proteins [2]. A minimal glycoepitope required for selectin binding is the sialyl Lewis X structure (sLe^X; Neu5Acα2-3Galβ1-4(Fucα1,3)GlcNAcβ1-R) [8,28,29]. The sLe^X can cap N-/O-glycans on many proteins and glycans on lipids [8]. Below we consider O- and N-glycosylation processes separately.

The total expression of genes encoding enzymes involved in O-glycosylation in the control cultured SKOV3 cells and SKOV3-derived tumors were 1.7 and 1.5-fold higher than that in the respective OVCAR8 samples. c-Fos overexpression led to 1.9 and 1.6-fold downregulation in SKOV3 cultured cells and tumors, respectively. Thus, the expression levels of the *GALNT12*, *GALNT14* and *GCNT3* genes decreased 4.8, 4.9 and 13.9 times in SKOV3 tumors, respectively. In OVCAR8 cultured cells and tumors, there were no significant changes in the expression levels of O-glycosylation genes. As a result, the total amount of mRNA from O-glycosylation genes in SKOV3 tumors with c-Fos overexpression was close to that in OVCAR8 tumors.

Since some of the enzymes can substitute for others in terms of activity, the changes in expression levels of individual genes may not correlate with the level of glycosylation. To account for this possible discrepancy, we considered several groups of O-glycosylation enzyme genes according to each step of O-glycan synthesis in the cells. Of the variety of possible structures of O-linked oligosaccharides, for further consideration, we chose a part of the process of O-glycan synthesis that is the most important in terms of tumor aggressiveness [29]. In particular, we focused on the synthesis of the Tn antigen and the structures of Core 1, Core 2, Core 3, and Core 4 (Fig. 2). For each step of the synthesis (i = 1, 2, 3 …), the k_i coefficient was introduced to represent the number of enzymes taking part in that step. We based this hypothesis on the observation that the amount of protein in the tumor cell was proportional to the amount of mRNA of the respective gene in accordance with [30]:

$$k_i = \sum E_{tumor\ cell},$$

when $\sum E_{tumor\ cell}$ – a sum of expression levels (Affymetrix microarray units) of genes encoding enzymes performing the i-th step of O-linked oligosaccharides. Here we use the assumption that the activities of all enzymes of the i-th step are nearly the same.

Based on [29,30], we identified five steps of O-linked oligosaccharides. For each of the five steps, the respective k_i coefficient was calculated:

k_1 – Tn antigen synthesis: *GALNT1, GALNT2, GALNT3, GALNT4, GALNT5, GALNT6, GALNT7, GALNT9, GALNT10, GALNT11, GALNT12, GALNT13, GALNT14, GALNTL1 (GALNT16), GALNTL2 (GALNT15), GALNTL4 (GALNT18), GALNTL5,* and *WBSCR17*;
k_2 – Core 1 structure synthesis: *C1GALT1* and *C1GALT1C1*;
k_3 – Core 3 structure synthesis: *B3GNT6*;
k_4 – Core 2 structure synthesis: *GCNT1, GCNT2,* and *GCNT3*;
k_5 – Core 4 structure synthesis: *GCNT2* and *GCNT3*.

The gene expression levels and the values of all five coefficients are presented in Additional file 3: Table S3.

Then, we calculated the fold changes of the coefficient values comparing control and c-Fos-overexpressing OVCAR8 and SKOV3 samples (Table 3).

The results presented in Table 3 show that SKOV3 cells significantly differed from OVCAR8 cells in the expression of genes encoding enzymes that perform the second, fourth and fifth steps of O-glycan synthesis (from 2 to 9 times). The amounts of mRNA encoding the enzymes of the fourth and fifth steps were higher while the amounts of mRNA encoding the enzymes of the second step were lower in SKOV3 cells than in OVCAR8 cells. In response to

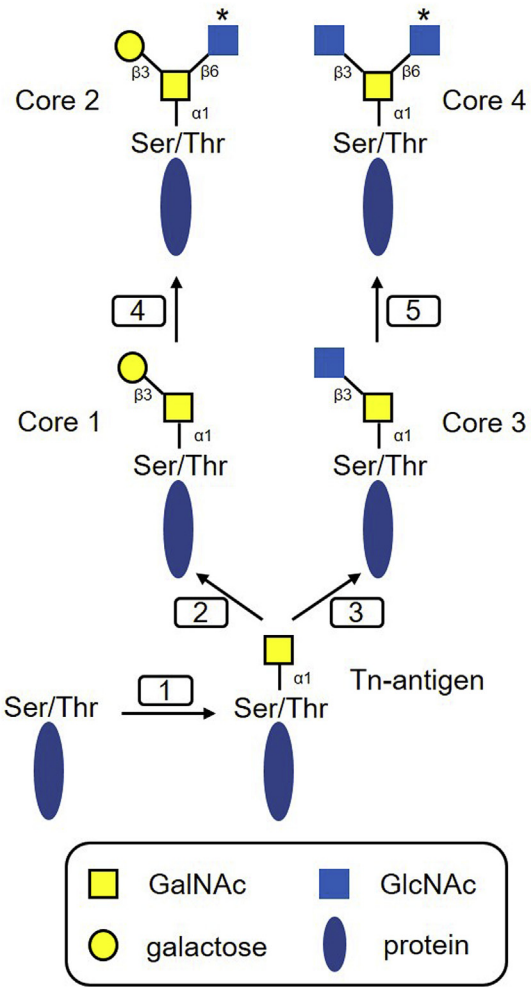

Fig. 2. Scheme of O-linked oligosaccharide synthesis. The numbers under the arrows represent the steps of synthesis used for the respective coefficient calculations. Asterisks mark the saccharide residue that can be capped by sLe^X.

Table 3
Expression level differences of groups of genes performing each of the five steps of O-linked oligosaccharide synthesis. The values of the ratios of respective coefficients are presented (fold changes: FCs).

Type of samples	Type of sample comparison	FC[a]				
		k_1	k_2	k_3	k_4	k_5
Cells	OVCAR8-cFos/OVCAR8-control	0.9	0.9	1.0	1.0	1.4
	SKOV3-cFos/SKOV3-control	0.7	0.7	1.4	**0.2**	**0.1**
	SKOV3-control/OVCAR8-control	1.1	**0.5**	1.0	**4.6**	**9.1**
	SKOV3-cFos/OVCAR8-*c*-Fos	1.0	**0.4**	1.4	1.0	1.0
Tumors	OVCAR8-cFos/OVCAR8-control	0.9	1.0	1.1	1.1	1.3
	SKOV3-cFos/SKOV3-control	0.8	0.9	1.1	**0.1**	**0.1**
	SKOV3-control/OVCAR8-control	1.3	0.8	1.0	**4.3**	**8.3**
	SKOV3-cFos/OVCAR8-*c*-Fos	1.2	0.7	1.0	**0.6**	0.7

[a] FC values indicating upregulation or downregulation of gene groups of 1.5 times or more are indicated in bold.

c-Fos overexpression, the expression levels of the enzyme-coding genes of the fourth and fifth steps fell substantially in SKOV3 cells, while no significant changes in the expression of these genes were observed in OVCAR8 cells. As a result, the amounts of enzymes of the respective steps in SKOV3 cells became comparable to those of OVCAR8 cells. Of note, the enzymes of the fourth and fifth O-glycan synthesis steps lead to the formation of the sLe^X precursor structure (Fig. 2).

Similar to the differences observed in SKOV3 and OVCAR8 cells, SKOV3- and OVCAR8-derived tumors also exhibited significant differences in the gene expression levels of the enzymes of the fourth and fifth O-glycan synthesis steps. Almost no changes in the expression levels of the enzymes of any of the steps in O-glycan synthesis were observed in OVCAR8 tumors in response to c-Fos overexpression. c-Fos overexpression in SKOV3 tumors caused substantial reductions in the mRNA levels of enzymes performing the fourth and fifth O-glycan synthesis steps. The amount of enzyme-coding mRNAs of the fourth step in SKOV3 tumors was decreased 1.7-fold compared with that in OVCAR8 tumors.

The total mRNA levels of genes encoding enzymes involved in N-glycosylation of cellular proteins were similar in control SKOV3 and OVCAR8 cultured cells and tumors. c-Fos overexpression did not cause any significant changes in the total amount of these mRNAs in any of the sample types. Such a lack of sensitivity to c-Fos overexpression of the genes encoding N-glycosylation enzymes could be explained by the large number of N-glycosylation enzymes, in contrast to O-glycosylation enzymes, that operate in the endoplasmic reticulum (about half of all enzymes involved in N-glycosylation) and play a crucial role in glycosylation of 50% of cellular proteins as well as in maintaining cellular homeostasis [30,31]. N-glycosylation is characterized by a large variety of possible oligosaccharide structures. Below we consider the gene expression of the enzymes specifically involved in the synthesis of complex type N-linked oligosaccharides (Fig. 3), which is the most common type of N-glycans [30]. Enzymes involved in the synthesis of this type of oligosaccharides function in the Golgi apparatus or on the cell surface. The complex type N-linked oligosaccharides are also the most important N-glycans in terms of the aggressiveness of tumor cells [29].

For enzymes involved in the synthesis of the complex N-linked oligosaccharides, we performed the coefficient calculation using the same procedure that was used for the O-glycosylation enzymes. The process of synthesis was divided into five sequential steps ($i = 1 \ldots, 5$). For each step, a coefficient representing the total expression of genes encoding enzymes involved in that step was calculated:

k_1 – *MAN2A1* and *MAN2A2*;
k_2 – *FUT8*;
k_3 – *MGAT2*;
k_4 – *MGAT3*;
k_5 – *MGAT5* and *MGAT5B*.

The gene expression levels and the values of all five coefficients are presented in Additional file 4: Table S4.

Then, we calculated the FCs of the coefficient values comparing control and c-Fos-overexpressing OVCAR8 and SKOV3 samples (Table 4).

The results presented reveal that the mRNA levels of the genes encoding enzymes involved in the first, third and fifth steps are comparable in control SKOV3 and OVCAR8 cells. For the enzymes of the second and fourth steps, the mRNA levels were 1.6- and 2-fold higher, respectively in control SKOV3 cells than in control OVCAR8s cells. c-Fos overexpression caused downregulation of genes encoding enzymes performing the second and fourth steps in SKOV3 cells, while c-Fos overexpression in OVCAR8 cells did not cause any significant changes in the expression levels of these genes. As a result, the mRNA levels of genes encoding enzymes involved in all but the second step of synthesis in SKOV3 cells became similar to those in OVCAR8 cells. The second step includes

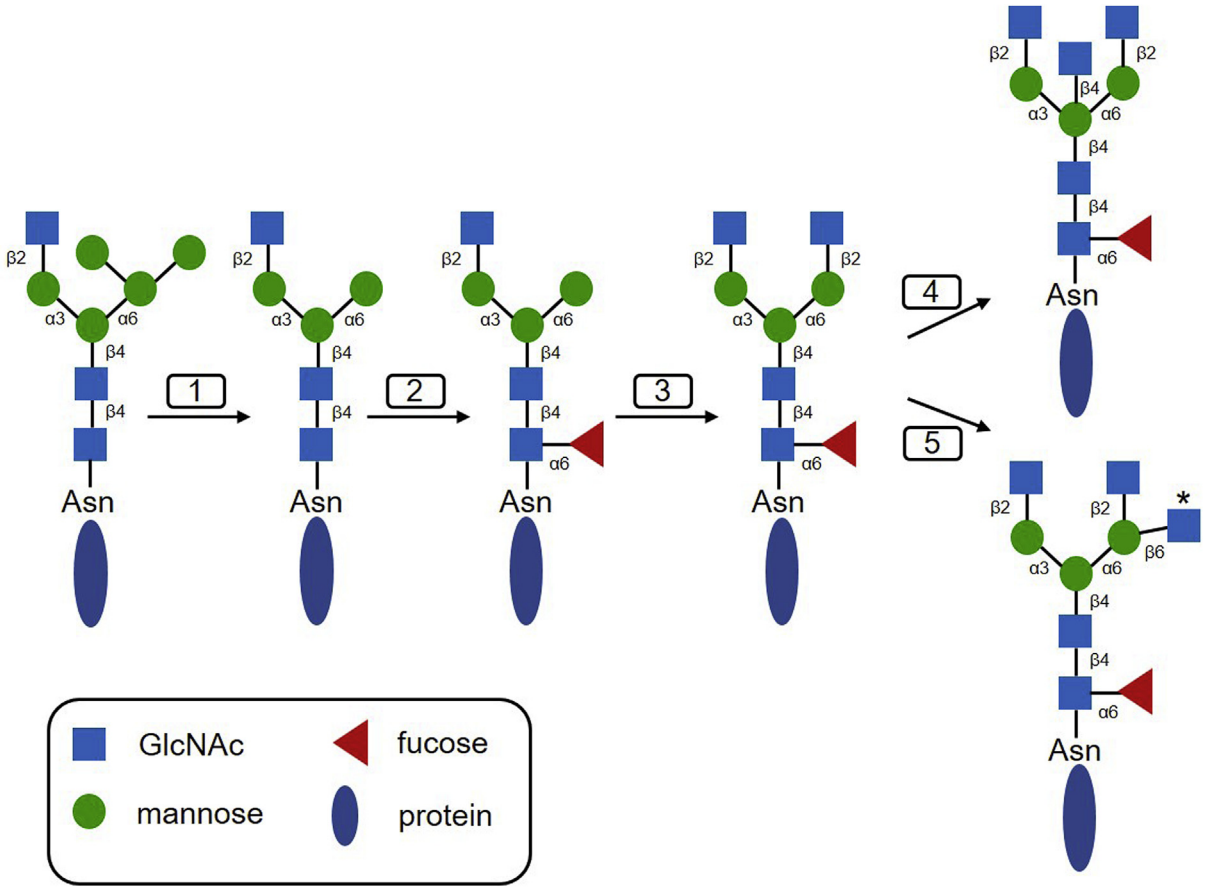

Fig. 3. Scheme of complex type N-linked oligosaccharide synthesis. The numbers under the arrows represent the steps of synthesis used for the respective coefficient calculations. Asterisks mark the terminal GclNAc residue that can be capped by sLe^X.

only the *FUT8* gene, the expression of which was 1.9 times lower in SKOV3 cells.

In control tumors, the mRNA levels of the genes encoding enzymes involved in all but the fourth step of complex type N-glycan synthesis were similar between SKOV3 and OVCAR8 samples. The mRNA expression levels of the genes encoding enzymes involved in the fourth step were 2.4 times higher in SKOV3 control tumors than in OVCAR8 control tumors. In OVCAR8 tumors, c-Fos overexpression did not lead to changes in the mRNA levels of genes encoding enzymes involved in any step of synthesis. However, in SKOV3 tumors, overexpression of the transcription factor was associated with 1.6-, 2-, and 1.6-fold downregulation of the expression of the enzymes involved in the first, fourth and fifth steps, respectively. As a result, similar to the cell samples, the mRNA levels of the genes encoding enzymes involved in all but the first step of synthesis were comparable between SKOV3 and OVCAR8 tumors. The mRNA expression levels of the genes encoding enzymes involved in the first step were 1.7 times lower in SKOV3-cFos tumors than in OVCAR8 tumors. Of note, the enzymes of the fifth step, the expression levels of which were downregulated in SKOV3-*c*-Fos tumors compared with those in OVCAR8 tumors, function in the formation of an N-glycan structure that can be capped by sLe^X.

Tetrasaccharide sLe^X (Fig. 4) is a crucial component of the glycosylation of tumor cell surface proteins that allows them to serve as ligands for selectins [28,29]. As mentioned above, sLe^X can cap both O- and N-glycans [8]. The sugar residues relevant to this process are specified in Figs. 2 and 3.

For enzymes involved in the synthesis of the sLe^X structure, we performed the coefficient calculation using the same procedure that was used for the O- and N-glycosylation enzymes. The process of sLe^X synthesis was divided into five sequential steps ($i = 1 \ldots,5$) according to [30,32–35]. For each step, the coefficient representing the total expression of genes encoding enzymes performing that step was calculated:

k_1 – *B4GALT1, B4GALT2, B4GALT3, B4GALT4, B4GALT5,* and *B4GALT7*;
k_2 – *B3GNT1, B3GNT2, B3GNT4, B3GNT5,* and *B3GNT8*;

Table 4
Expression level differences of groups of genes performing each of the five steps of complex type N-linked oligosaccharide synthesis. The values of the ratios of respective coefficients are presented (fold changes: FCs).

Type of samples	Type of sample comparison	FC[a]				
		k_1	k_2	k_3	k_4	k_5
Cells	OVCAR8-cFos/OVCAR8-control	0.9	0.9	1.2	1.1	0.9
	SKOV3-cFos/SKOV3-control	0.9	**0.3**	1.0	0.7	1.0
	SKOV3-control/OVCAR8-control	0.9	**1.6**	0.9	**2.0**	0.9
	SKOV3-cFos/OVCAR8-*c*-Fos	0.8	**0.5**	0.8	1.4	1.0
Tumors	OVCAR8-cFos/OVCAR8-control	1.2	1.3	1.3	1.0	0.9
	SKOV3-cFos/SKOV3-control	**0.6**	0.8	1.2	**0.5**	**0.6**
	SKOV3-control/OVCAR8-control	1.1	1.3	1.2	**2.4**	1.2
	SKOV3-cFos/OVCAR8-*c*-Fos	**0.6**	0.9	1.1	1.2	0.9

[a] FC values indicating upregulation or downregulation of gene groups of 1.5 times or more are indicated in bold.

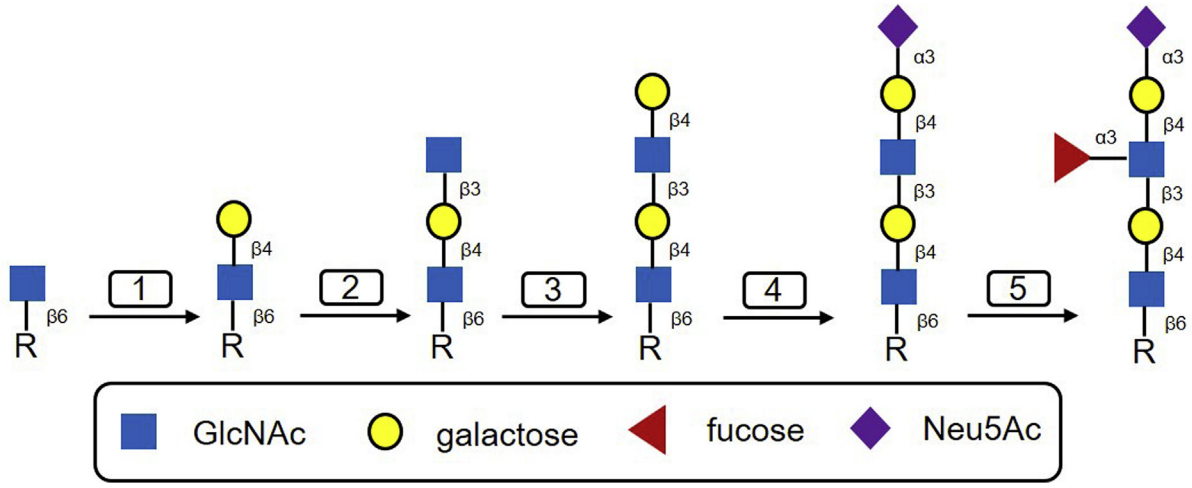

Fig. 4. The scheme of sialyl Lewis X (sLe^X) synthesis. The numbers under the arrows represent the steps of synthesis used for the respective coefficient calculations. R – the terminal GclNAc residue marked by an asterisk in Figs. 2 and 4.

k_3 – *B4GALT1*, *B4GALT2*, *B4GALT3*, *B4GALT4*, *B4GALT5*, and *B4GALT7*;
k_4 – *ST3GAL3*, *ST3GAL4*, and *ST3GAL6*;
k_5 – *FUT3*, *FUT4*, *FUT5*, *FUT6*, *FUT7*, *FUT9*, *FUT10*, and *FUT11*.

The gene expression levels and the values of all five coefficients are presented in Additional file 5: Table S5.

Then, as for the O- and N-glycosylation enzymes, we calculated the FCs of the coefficient values comparing control and c-Fos-overexpressing OVCAR8 and SKOV3 samples (Table 5).

The results presented reveal that c-Fos overexpression did not significantly change the expression of the enzymes at any step of sLe^X synthesis in OVCAR8 cells and OVCAR8 tumors. In SKOV3 cells, there were only partial changes in response to c-Fos overexpression. However, in SKOV3 tumors, upregulation of the enzymes involved in the second step (1.8-fold) and downregulation (1.7-fold) of the enzymes involved in the fifth step were observed. The control cells and tumors showed comparable expression levels of all enzymes except for the enzymes involved in the second step of synthesis, which were 1.7 and 1.8 times higher, respectively, in the SKOV3 samples, and the enzymes involved in the fifth step of synthesis, which were slightly upregulated in the SKOV3 samples. After c-Fos overexpression, the expression levels of the enzymes involved in the first, third, and fifth steps were comparable in SKOV3 and OVCAR8 tumors. The genes involved in the second step were expressed at even higher levels in SKOV3 tumors. The genes involved in the fourth step were expressed at levels 1.6-fold lower in SKOV3 tumors than in OVCAR8 samples. It is interesting to note that the *ST3GAL6* gene encoding one of the two most important sialyltransferases of the fourth step of sLe^X synthesis [32,34,36] was not expressed in OVCAR8 samples (see Table S5). This suggests that sLe^X was either absent or present at very low levels in OVCAR8 samples (both cells and tumors). In contrast, sLe^X was present in control SKOV3 tumors, and c-Fos overexpression significantly reduced or totally abolished sLe^X levels. This observation is consistent with previously obtained flow cytometry data from cultured cells [15].

Table 5
Expression level differences of groups of genes performing each of the five steps of the tetrasaccharide sialyl Lewis X (sLe^X) synthesis. The values of the respective coefficient ratios are presented (fold changes: FCs).

Type of samples	Type of sample comparison	FC[a]				
		k_1	k_2	k_3	k_4	k_5
Cells	OVCAR8-cFos/OVCAR8-control	1.1	1.0	1.1	1.0	0.8
	SKOV3-cFos/SKOV3-control	0.9	1.1	0.9	0.9	0.8
	SKOV3-control/OVCAR8-control	0.9	**1.7**	0.9	0.8	1.3
	SKOV3-cFos/OVCAR8-*c*-Fos	0.8	1.8	0.8	0.8	1.4
Tumors	OVCAR8-cFos/OVCAR8-control	1.0	1.1	1.0	1.0	0.8
	SKOV3-cFos/SKOV3-control	0.9	**1.8**	0.9	0.8	**0.6**
	SKOV3-control/OVCAR8-control	1.0	**1.9**	1.0	0.8	1.4
	SKOV3-cFos/OVCAR8-*c*-Fos	0.9	**3.1**	0.9	**0.6**	1.1

[a] FC values indicating upregulation or downregulation of gene groups of 1.5 times or more are indicated in bold.

4. Discussion

In our previous study, we have demonstrated that primary tumor growth, number of circulating tumor cells, and number of spontaneous lung metastases has been reduced in SCID mice injected with c-Fos-overexpressing SKOV3 cells in comparison with that in mice injected with control SKOV3 cells [15]. This observation is mirrored in clinical studies in which high expression of c-Fos in tumors is associated with favorable prognosis and longer recurrence-free and overall survival in OvCa patients [13], a correlation which stresses the clinical relevance of our model. In the present study, we found that overexpression of c-Fos in OVCAR8 cells, which is also a human OvCa cell line, did not alter cancer progression in SCID mice injected with the cells. This discrepancy needed to be explained as understanding of molecular mechanisms underlying this unexpected finding might facilitate understanding of malignant progression in OvCa.

Intraperitoneal metastasis facilitated by the circulation of peritoneal fluid is the main route of OvCa progression, although hematogenous and lymphatic metastasis also occurs [10]. Potential mechanisms for the attachment of OvCa cells to the peritoneal surfaces include both binding of selectin ligands on tumor cells with selectins on the mesothelium [9] and binding to extracellular matrix proteins (e.g. collagen type I and IV, laminins, and fibronectin) expressed on the surface of human peritoneal mesothelial cells via integrins [10–12]. Mesothelial and endothelial cells express E- and P-selectins and it had been shown that SKOV3 cells attach to endothelial and mesothelial monolayers in *in vitro* assays mimicking physiological conditions in leukocyte transmigration [15]. Overexpression of c-Fos in SKOV3 and, to a lesser extent,

OVCAR8 cells lead to decrease in adhesion to endothelial and mesothelial surfaces [15]. It has been hypothesized that, along with other cancer cells and leukocytes, SKOV3 cells mainly use the selectin-dependent leukocyte-like adhesion cascade for attachment to peritoneal and endothelial surfaces during metastasis.

The majority of cell membrane selectin ligands contains sLe^X structures that are terminal carbohydrate residues of both N-/O-glycans on many proteins and are crucial for the binding [8,28,29]. Unlike SKOV3 cells, OVCAR8 cells express little if any sLe^X as shown using flow cytometry [15]. Indeed, as mentioned above in contrast to strong adhesion of SKOV3 cells, OVCAR8 cells show only weak adhesion to selectin-expressing endothelial cells [15]. Since sLe^X represents the canonical selectin ligand, we compared expression of the sLe^X synthesizing enzymes in the OvCa cultured cells and tumors. Samples of OVCAR8 tumors and, to a lesser extent, cultured cells exhibited significantly lower amounts of mRNAs encoding the enzymes than corresponding SKOV3 samples, especially for enzymes involved in the fourth and the firth steps of O-linked oligosaccharide synthesis and in the second and fourth steps of N-linked oligosaccharide synthesis (Tables 3 and 4; Figs. 2 and 3). Both cultured SKOV3 cells and SKOV3-derived tumors showed dramatic decrease in expression of O-glycosylation enzymes of the forth and the firth steps and N-glycosylation enzymes of the first and the second steps in response to c-Fos overexpression. The change correlated with the reduced aggressiveness of SKOV3-derived tumors. Interestingly, expression of the glycosylation enzymes in OVCAR8 tumors and, to a lesser extent, in cultured OVCAR8 cells was even slightly increased in response to c-Fos overexpression. Low expression of selectin ligands suggests that the progression of OVCAR8 tumors might not rely on the selectin-dependent leukocyte-like adhesion cascade.

Molecular mechanisms of rolling, adhesion, and diapedesis (Fig. 1) through the endothelial and peritoneal surfaces are somewhat similar for leukocytes and tumor cells [4]. Binding to extracellular matrix proteins (ECM) or their receptors is another potential mechanism of initial adhesion of cancer cells to the peritoneum that might be a crucial step in OvCa progression. There are several findings supporting this hypothesis. It has been demonstrated that leukocytes show α6β1 integrin-mediated tethering and arrest on laminin under physiological shear flow [37]. Interaction of α6β4 integrin with laminin supports tethering and rolling of human breast epithelial and several types of carcinoma cells [38]. Interestingly, integrin-ligand interactions can be activated by shear stress and operate even as catch and bonds [39–43]. It has been shown that β1 integrin mediates binding of head and neck squamous cell carcinoma cells to laminin and the interaction is enhanced under shear stress [41]. Taken together, we suggest that the initial attachment of OVCAR8 cells to peritoneal mesothelium occurs predominantly through interactions of integrins (e.g. integrins comprising subunits encoded by *ITGA3*, *ITGA5*, *ITGA6*, *ITGAV*, *ITGB1*, *ITGB4*, *ITGB5,* and *ITGB8* genes) with ECM proteins.

Interestingly, c-Fos overexpression in SKOV3 cells but not in OVCAR8 cells decreases adhesion to ECM protein laminin-111 [15]. Noteworthy, the overall expression of laminin chains was similar in SKOV3 and OVCAR8 specimens (Additional file 6: Table S6) with the only exception of laminin α chain expression levels, which were strikingly different. Out of five laminin α chains known to date, SKOV3 cells and SKOV3-derived tumors expressed only α3 and α5 chains (Additional file 6: Table S6). c-Fos overexpression decreased the expression levels of α3 and α5 in both SKOV3 cells and SKOV3-derived tumors. Neither OVCAR8 cells nor OVCAR8-derived tumors expressed α3 laminin chain, but expression of laminin α1 and α5 chains was detected in all OVCAR8 specimens (Additional file 6: Table S6). c-Fos overexpression only slightly affected the expression levels of the laminin α chains in OVCAR8 cells and tumors. Laminins are able to bind to cell membrane receptors strongly affecting cellular behavior and the binding is mainly dependent on interactions between the cell and globular domains at the C terminus of laminin α chains [44]. Since OVCAR8 cells stably express laminins and laminin cellular membrane receptors such as integrins, it is possible that the cancer progression might depend on adhesion to and migration on the endogenously produced basement membranes.

According to SABiosciences' database, a promoter of *LAMC2* gene encoding γ2 laminin chain contains AP-1 transcription factor binding sites [45]. Indeed, c-Fos overexpression induced changes of *LAMC2* gene expression in both SKOV3 and OVCAR8 specimens, however in different directions. OVCAR8 cells and OVCAR8-derived tumors showed 3 and 6 times increase of γ2 chain mRNA level, respectively. There is only one laminin trimer, laminin-332, that contains γ2 chain [44]. As OCVAR8 cells lacked α3 laminin chain expression, OVCAR8 cells and tumors presumably produced γ2 chain as a monomer. Expression of γ2 monomer has been shown in many invasive tumors and is considered as a marker of invasive tumor phenotype [46,47]. Overexpression of c-Fos in SKOV3 cells and tumors was associated with decrease in laminin γ2 chain expression level (in 2.6–3 times) as well as with decrease in expression of genes encoding the two other chains comprising laminin-332 (*LAMA3* and *LAMB3* genes). Laminin-332 is heavily involved in cell adhesion, migration, and survival of various types of carcinomas [48,49] suggesting that laminins might also be involved in SKOV3-derived tumor metastasis.

Molecular mechanisms underlying progression of OvCa is not clear and involvement of laminins and their receptors in OvCa metastasis is still speculative. Analysis of prognostic significance of laminin chains and laminin receptors in patients with OvCa will be helpful for elucidation of their involvement in progression of the disease. Knock-out of genes encoding α1 and α3 laminin chains and their receptors in OVCAR8 and SKOV3 cells, respectively, will allow to test the importance of the laminins in metastasis. Xenograft experiments with selectin-deficient mice will allow to further clarify the importance of selectin and laminin pathways in OvCa progression.

5. Conclusions

High expression of c-Fos in ovarian cancer cells is not always associated with reduced metastatic potential. Low expression of the selectin-dependent leukocyte-like adhesion cascade genes and selectin ligands may not always affect progression of ovarian cancer. We suggest that ovarian cancer cells sustain a high metastatic potential via a selectin-independent pathway, presumably involving extracellular matrix proteins and/or their receptors.

Funding

This work was supported by a grant from The Russian Scientific Foundation (Grant 17-14-01338).

Availability of data and materials

The microarray datasets generated and analyzed during the current study are available in the NCBI's Gene Expression Omnibus repository and are accessible through GEO Series accession number GSE97226 (https://www.ncbi.nlm.nih.gov/geo/query/acc.cgi?acc=GSE97226).

Author contributions

Conception and design of the experiments: AGT, KM-LS, and US.

Collection of the data: DVM, NAK, LO-F, and CS. Analysis and interpretation of the data: DVM, SR, NAK, LO-F, and CS. Drafting and critically revising the article: DVM, SR, JAM, US, and AGT. All authors read and approved the final manuscript.

Competing interests

The authors declare that they have no competing interests.

Ethics approval and consent to participate

The methodology used to conduct the animal experiments was consistent with the UKCCCR guidelines for the welfare and use of animals in cancer research [15]. The experiment was recommended and supervised by the institutional animal welfare officer, and the local licensing authority (Behörde für Soziales, Familie, Gesundheit und Verbraucherschutz, Amt für Lebensmittelsicherheit und Veterinärwesen, Hamburg, Germany) approved of the experiment and assigned the project No. G09/58.

Acknowledgements

We thank Dr. Vladimir V. Galatenko and Irina A. Mityakina for their help with microarray data processing and bioinformatic data analysis, Dr. Timur Samatov for the fruitful discussions and helpful advice.

Appendix B. Supplementary data

Supplementary data related to this article can be found at https://doi.org/10.1016/j.biochi.2017.09.009.

References

[1] S. Köhler, S. Ullrich, U. Richter, U. Schumacher, E-/P-selectins and colon carcinoma metastasis: first *in vivo* evidence for their crucial role in a clinically relevant model of spontaneous metastasis formation in the lung, Br. J. Cancer 102 (2010) 602–609.
[2] K. Ley, C. Laudanna, M.I. Cybulsky, S. Nourshargh, Getting to the site of inflammation: the leukocyte adhesion cascade updated, Nat. Rev. Immunol. 7 (9) (2007) 678–689.
[3] N. Reymond, B.B. d'Água, A.J. Ridley, Crossing the endothelial barrier during metastasis, Nat. Rev. Cancer 13 (12) (2013) 858–870.
[4] C. Strell, F. Entschladen, Extravasation of leukocytes in comparison to tumor cells, Cell Commun. Signal. 6 (2008) 10.
[5] R.P. McEver, C. Zhu, Rolling cell adhesion, Annu. Rev. Cell Dev. Biol. 26 (2010) 363–396.
[6] P.L. Tremblay, J. Huot, F.A. Auger, Mechanisms by which E-selectin regulates diapedesis of colon cancer cells under flow conditions, Cancer Res. 68 (13) (2008) 5167–5176.
[7] L. Xia, M. Sperandio, T. Yago, J.M. McDaniel, R.D. Cummings, et al., P-selectin glycoprotein ligand-1-deficient mice have impaired leukocyte tethering to E-selectin under flow, J. Clin. Investig. 109 (2002) 939–950.
[8] A. Zarbock, K. Ley, R.P. McEver, A. Hidalgo, Leukocyte ligands for endothelial selectins: specialized glycoconjugates that mediate rolling and signaling under flow, Blood 118 (26) (2011) 6743–6751.
[9] Gebauer F1, D. Wicklein, K. Stübke, N. Nehmann, A. Schmidt, J. Salamon, K. Peldschus, M.F. Nentwich, G. Adam, G. Tolstonog, et al., Selectin binding is essential for peritoneal carcinomatosis in a xenograft model of human pancreatic adenocarcinoma in pfp−/rag2− mice, Gut 62 (2012) 741–750.
[10] D.S. Tan, R. Agarwal, S.B. Kaye, Mechanisms of transcoelomic metastasis in ovarian cancer, Lancet. Oncol. 7 (11) (2006) 925–934.
[11] R.S. Cotran, M.J. Karnovsky, Ultrastructural studies on the permeability of the mesothelium to horseradish peroxidase, J. Cell Biol. 37 (1) (1968) 123–137.
[12] Wassil Wassilev, Thilo Wedel, Krassimira Michailova, Wolfgang Kühnel, A scanning electron microscopy study of peritoneal stomata in different peritoneal regions, Ann. Anat. - Anat. Anz. 180 (2) (1998) 137–143.
[13] S. Mahner, C. Baasch, J. Schwarz, S. Hein, L. Wölber, F. Jänicke, K. Milde-Langosch, C-Fos expression is a molecular predictor of progression and survival in epithelial ovarian carcinoma, Br. J. Cancer 99 (8) (2008) 1269–1275.
[14] A.A. Poloznikov, A.A. Zakhariants, S.V. Nikulin, N.A. Smirnova, D.M. Hushpulian, I.N. Gaisina, A.G. Tonevitsky, V.I. Tishkov, I.G. Gazaryan, Structure-activity relationship for branched oxyquinoline HIF activators: Effect of modifications to phenylacetamide "tail", Biochimie 133 (2017) 74–79.
[15] L. Oliveira-Ferrer, K. Rößler, V. Haustein, C. Schröder, D. Wicklein, D. Maltseva, N. Khaustova, T. Samatov, A. Tonevitsky, S. Mahner, F. Jänicke, U. Schumacher, K. Milde-Langosch, c-FOS suppresses ovarian cancer progression by changing adhesion, Br. J. Cancer 110 (3) (2014) 753–763.
[16] P. Workman, E.O. Aboagye, F. Balkwill, A. Balmain, G. Bruder, D.J. Chaplin, J.A. Double, J. Everitt, D.A. Farningham, M.J. Glennie, L.R. Kelland, V. Robinson, I.J. Stratford, G.M. Tozer, S. Watson, S.R. Wedge, S.A. Eccles, Committee of the National Cancer Research Institute, Guidelines for the welfare and use of animals in cancer research, Br. J. Cancer 102 (11) (2010) 1555–1577.
[17] N. Nehmann, D. Wicklein, U. Schumacher, R. Müller, Comparison of two techniques for the screening of human tumor cells in mouse blood: quantitative real-time polymerase chain reaction (qRT-PCR) versus laser scanning cytometry (LSC), Acta Histochem. 112 (5) (2010) 489–496.
[18] D.V. Maltseva, N.A. Khaustova, N.N. Fedotov, E.O. Matveeva, A.E. Lebedev, M.U. Shkurnikov, V.V. Galatenko, U. Schumacher, A.G. Tonevitsky, High-throughput identification of reference genes for research and clinical RT-qPCR analysis of breast cancer samples, J. Clin. Bioinforma. 3 (1) (2013) 13.
[19] Alexander G. Tonevitsky, Diana V. Maltseva, Asghar Abbasi, Timur R. Samatov, Dmitry A. Sakharov, Maxim U. Shkurnikov, Alexey E. Lebedev, Vladimir V. Galatenko, Anatoly I. Grigoriev, Hinnak Northoff, Dynamically regulated miRNA-mRNA networks revealed by exercise, BMC Physiol. 13 (1) (2013) 9.
[20] Affymetrix® Expression Console™ Software 1.4 User Manual. ©Affymetrix, Inc. 2014. http://media.affymetrix.com/support/downloads/manuals/expression_console_userguide.pdf.
[21] R.A. Irizarry, B. Hobbs, F. Collin, Y.D. Beazer-Barclay, K.J. Antonellis, U. Scherf, T.P. Speed, Exploration, normalization, and summaries of high density oligonucleotide array probe level data, Biostat. Oxf. Engl. 4 (2) (2003) 249–264.
[22] D.V. Maltseva, V.V. Galatenko, T.R. Samatov, S.O. Zhikrivetskaya, N.A. Khaustova, I.N. Nechaev, M.U. Shkurnikov, A.E. Lebedev, I.A. Mityakina, A.D. Kaprin, et al., miRNome of inflammatory breast cancer, BMC Res. Notes 7 (1) (2014) 871.
[23] S. Aigner, C.L. Ramos, A. Hafezi-Moghadam, M.B. Lawrence, J. Friederichs, P. Altevogt, K. Ley, CD24 mediates rolling of breast carcinoma cells on P-selectin, FASEB J. Off. Publ. Fed. Am. Soc. Exp. Biol. 12 (12) (1998) 1241–1251.
[24] M.R. Dallas, S.H. Chen, M.M. Streppel, S. Sharma, A. Maitra, K. Konstantopoulos, Sialofucosylated podocalyxin is a functional E- and L-selectin ligand expressed by metastatic pancreatic cancer cells, Am. J. Physiol. Cell Physiol. 303 (6) (2012) C616–C624.
[25] Y. Geng, J.R. Marshall, M.R. King, Glycomechanics of the metastatic cascade: tumor cell-endothelial cell interactions in the circulation, Ann. Biomed. Eng. 40 (4) (2012) 790–805.
[26] A. Hidalgo, A.J. Peired, M. Wild, D. Vestweber, P.S. Frenette, Complete identification of E-selectin ligands on neutrophils reveals distinct functions of PSGL-1, ESL-1, and CD44, Immunity 26 (4) (2007) 477–489.
[27] Y. Katayama, A. Hidalgo, J. Chang, A. Peired, P.S. Frenette, CD44 is a physiological E-selectin ligand on neutrophils, J. Exp. Med. 201 (8) (2005) 1183–1189.
[28] C.A. St Hill, Interactions between endothelial selectins and cancer cells regulate metastasis, Front. Biosci. Landmark Ed. 16 (2011) 3233–3251.
[29] T. Lange, T.R. Samatov, A.G. Tonevitsky, U. Schumacher, Importance of altered glycoprotein-bound N- and O-glycans for epithelial-to-mesenchymal transition and adhesion of cancer cells, Carbohydr. Res. 389 (2014) 39–45.
[30] A.V. Nairn, W.S. York, K. Harris, E.M. Hall, J.M. Pierce, K.W. Moremen, Regulation of glycan structures in animal tissues: transcript profiling of glycan-related genes, J. Biol. Chem. 283 (25) (2008) 17298–17313.
[31] E.M. Comelli, S.R. Head, T. Gilmartin, T. Whisenant, S.M. Haslam, S.J. North, N.K. Wong, T. Kudo, H. Narimatsu, J.D. Esko, K. Drickamer, A. Dell, J.C. Paulson, A focused microarray approach to functional glycomics: transcriptional regulation of the glycome, Glycobiology 16 (2) (2006) 117–131.
[32] F. Dall'Olio, N. Malagolini, M. Trinchera, M. Chiricolo, Sialosignaling: sialyltransferases as engines of self-fueling loops in cancer progression, Biochim. Biophys. Acta 1840 (9) (2014) 2752–2764.
[33] A.S. Carvalho, A. Harduin-Lepers, A. Magalhães, E. Machado, N. Mendes, L.T. Costa, R. Matthiesen, R. Almeida, J. Costa, C.A. Reis, Differential expression of alpha-2,3-sialyltransferases and alpha-1,3/4-fucosyltransferases regulates the levels of sialyl Lewis a and sialyl Lewis x in gastrointestinal carcinoma cells, Int. J. Biochem. Cell Biol. 42 (1) (2010) 80–89.
[34] A. Cazet, S. Julien, M. Bobowski, J. Burchell, P. Delannoy, Tumour-associated carbohydrate antigens in breast cancer, Breast Cancer Res. BCR 12 (3) (2010) 204.
[35] H. Kitagawa, J.C. Paulson, Cloning and expression of human Gal beta 1,3(4) GlcNAc alpha 2,3-sialyltransferase, Biochem. Biophys. Res. Commun. 194 (1) (1993) 375–382.
[36] T.1 Okajima, S. Fukumoto, H. Miyazaki, H. Ishida, M. Kiso, K. Furukawa, T. Urano, K. Furukawa, Molecular cloning of a novel α2, 3-sialyltransferase (ST3Gal VI) that sialylates type II lactosamine structures on glycoproteins and glycolipids, J. Biol. Chem. 274 (17) (1999) 11479–11486.
[37] Joji Kitayama, Shigeo Ikeda, Kyoko Kumagai, Hideaki Saito, Hirokazu Nagawa, α6β1 integrin (VLA-6) mediates leukocyte tether and arrest on laminin under physiological shear flow, Cell. Immunol. 199 (2) (2000) 97–103.
[38] A. Tozeren, H.K. Kleinman, S. Wu, A.M. Mercurio, S.W. Byers, Integrin α6β4 mediates dynamic interactions with laminin, J. Cell Sci. 107 (11) (1994) 3153–3163.
[39] S. Chakrabarti, M. Hinczewski, D. Thirumalai, Plasticity of hydrogen bond networks regulates mechanochemistry of cell adhesion complexes, Proc. Natl.

Acad. Sci. U. S. A. 111 (25) (2014) 9048–9053.
[40] W. Chen, J. Lou, C. Zhu, Forcing switch from short- to intermediate- and long-lived states of the alphaA domain generates LFA-1/ICAM-1 catch bonds, J. Biol. Chem. 285 (46) (2010) 35967–35978.
[41] S.M. Fennewald, C. Kantara, S.K. Sastry, V.A. Resto, Laminin interactions with head and neck cancer cells under low fluid shear conditions lead to integrin activation and binding, J. Biol. Chem. 287 (25) (2012) 21058–21066.
[42] J.C. Friedland, M.H. Lee, D. Boettiger, Mechanically activated integrin switch controls alpha5beta1 function, Sci. (New York, N.Y.) 323 (5914) (2009) 642–644.
[43] F. Kong, A.J. García, A.P. Mould, M.J. Humphries, C. Zhu, Demonstration of catch bonds between an integrin and its ligand, J. Cell Biol. 185 (7) (2009) 1275–1284.
[44] A. Domogatskaya, S. Rodin, K. Tryggvason, Functional diversity of laminins, Annu. Rev. Cell Dev. Biol. 28 (2012) 523–553.
[45] http://www.sabiosciences.com/chipqpcrsearch.php?species_id=0&factor=Over+200+TF&gene=lamc2&nfactor=n&ninfo=n&ngene=n&B2=Search.
[46] K. Miyazaki, Laminin-5 (laminin-332): unique biological activity and role in tumor growth and invasion, Cancer Sci. 97 (2) (2006) 91–98.
[47] K.H. Oh, J. Choi, J.S. Woo, S.K. Baek, K.Y. Jung, M.J. Koh, Y.-S. Kim, S.Y. Kwon, Role of laminin 332 in lymph node metastasis of papillary thyroid carcinoma, Auris Nasus Larynx (2017), https://doi.org/10.1016/j.anl.2017.01.010.
[48] M.P. Marinkovich, Tumour microenvironment: laminin 332 in squamous-cell carcinoma. Nat. Rev. Cancer 7 (5) (2007) 370–380.
[49] P. Rousselle, K. Beck, Laminin 332 processing impacts cellular behavior, Cell Adhes. Migr. 7 (1) (2013 Jan-Feb) 122–134.